General Disclaimer

One or more of the Following Statements may affect this Document

- This document has been reproduced from the best copy furnished by the organizational source. It is being released in the interest of making available as much information as possible.

- This document may contain data, which exceeds the sheet parameters. It was furnished in this condition by the organizational source and is the best copy available.

- This document may contain tone-on-tone or color graphs, charts and/or pictures, which have been reproduced in black and white.

- This document is paginated as submitted by the original source.

- Portions of this document are not fully legible due to the historical nature of some of the material. However, it is the best reproduction available from the original submission.

NASA Technical Memorandum 78797

ACOUSTIC HOLOGRAPHY - PROBLEMS ASSOCIATED WITH CONSTRUCTION AND RECONSTRUCTION TECHNIQUES

JAG J. SINGH

SEPTEMBER 1978

NASA
National Aeronautics and Space Administration

Langley Research Center
Hampton, Virginia 23665

INTRODUCTION

Holography, in its broadest sense, involves interference between a coherent reference radiation beam and another beam of coherent radiation scattered from an object under inspection. The radiation beams can be mechanical (as in the case of sound holography) or electromagnetic (as in the case of light holography). The interference pattern, upon interrogation by coherent radiation beam, yields detailed information about the scattering object. With the advent of the lasers, great progress has been made in the development of optical holography. There has not been a corresponding development in sound holography even though there have been powerful, coherent, sound sources at our disposal for a long time. And yet there are certain valid fields where acoustic holography is expected to play a very important role. For instance, sound propagation is still the best method for detecting and locating submerged objects for distances greater than a few kilometers. Easy propagation of sound waves through solids makes sound holography easily adaptable for nondestructive testing of solid devices and it is expected to be considerably cheaper and safer than, for example, neutron radiography. Medical diagnostic applications constitute yet another potential field, although sound propagation in tissues is far from being fully realized mainly because of the lack of adequate hologram recording and reconstruction techniques. It is the purpose of this report to review the status of sound holography and critically examine the status of sound-to-light conversion techniques. In the latter context, new and more fruitful areas of research will be identified.

GENERALIZED THEORY

Consider two mutually coherent and monochromatic radiation beams, $A(x,y)e^{-i\omega t}$ and $B(x,y)e^{-i\omega t}$, arriving at the receiver.(*) $A(x,y)$ and

---

(*)The interfering wave amplitudes have been expressed in the following simplified form in the x-y plane of the receiver:

$$U_1(r) = a\, e^{ik\cdot r}\, e^{-i(\omega t+\phi_1)}$$

$$= \left[a\, e^{i(k\cdot r-\phi_1)}\right] e^{-i\omega t}$$

$$= A(x,y,z)e^{-i\omega t} \equiv A(x,y)e^{-i\omega t}$$

and similarly

$$U_2(r) = B(x,y,z)e^{-i\omega t} \equiv B(x,y)e^{-i\omega t}$$

$B(x,y)$ represent the complex amplitudes of the two beams in the plane (x,y) of the receiver. In the case of squared-law detectors, the resultant recorded intensity at the receiver is given by

$$I = |A + B|^2$$

$$= (A + B)(A^* + B^*)$$

$$= (AA^* + BB^*) + (AB^* + A^*B) \qquad (1)$$

The first term represents the sum of individual intensities whereas the terms in the second bracket represent the interference phenomenon. In optics, it is possible to measure the entire second bracket whereas in sound or microwave holography, one can pick out AB^* or A^*B term singly. The recorded intensity I, as given by equation (1), represents the hologram at the receiver. In the case of a photographic recording medium, its amplitude transmission, T, is related to the intensity, I, as follows:

$$T = I^{-\gamma/2}$$

where γ is the slope of the emulsion response curve. To simplify explanation, it will be assumed that the photographic emulsion processing is such that $\gamma = -2$ and therefore transmission is proportional to I.

If now the recorded hologram is interrogated with either $A\,e^{-i\omega t}$ or $B\,e^{-i\omega t}$, one will get the remaining wave and its complex conjugate as seen below. The transmitted amplitude behind the hologram is given by the following expression:

$$A \cdot T \equiv A \cdot I$$

$$= A\,|A + B|^2$$

$$= A(AA^* + BB^*) + A(AB^* + A^*B) \qquad (2)$$

Leaving out the first bracket and confining attention to the second bracket which contains the signal bearing interference fringes,

$$A \cdot T = \text{Const} + AAB^{*} + AA^{*}B$$

(Twin Wave) (Reconstructed Wave)

In the case of two identical plane waves, B and B^{*} are reconstituted with unit magnification. If the two waves were spherical, the virtual image would still have unit magnification but the real image will have a magnification other than unity. (See figure 1 for general construction/reconstruction techniques in holography.)

In the case of a point object, the recorded hologram is a zone plate. In general, a surface hologram may be considered a generalized zone plate with a built-in object. Such a zone plate has two simultaneous focal lengths, $\pm f$.

$$\frac{1}{f} = \pm\left(\frac{1}{v} - \frac{1}{u}\right) \tag{4}$$

where u and v represent distance from the reference source to the hologram and the object source to the hologram, respectively.

These zone plates are characterized by two fundamental properties:

$$\left.\begin{aligned} d^{2} &\propto f\lambda \\ f\lambda &= \text{Constant} \end{aligned}\right\} \tag{5a}$$

where d represents the linear dimensions of the hologram and λ represents the constructing wavelength. [$\lambda = (k)^{-1}$.]

The discussion, so far, is equally applicable to the optical and sound holograms. However, one cannot use an acoustical wave to reconstruct an optically visible image. That is, in the case of an acoustical holograph, the interrogating beam will be different from the constructing beam. Let the interrogating wave be represented by $A'(x,y)e^{-i\omega' t}$. In this case, the transmitted amplitude behind the hologram is given by the following expression (ignoring the zero order terms):

$$A' \cdot T = (A' \cdot AB^{*} + A' \cdot A^{*}B)e^{-i\omega' t} \tag{5b}$$

As is obvious from the right-hand side terms and figure 1(c), there are still

two images, just as in the case of light-to-light holograms. However, the hologram acts like a lens having a modified focal length, f', given by:

$$f' = (m^2)\left[\frac{\lambda(\text{inspector})}{\lambda(\text{interrogator})}\right] f \qquad (5c)$$

where m = hologram scaling factor. Preservation of three-dimensionality in the reconstruction requires that the hologram scaling factor, m, be properly matched to the λ(interrogator/λ(inspector) ratio. (See Appendix.) In Gabor's original experiment (ref. 1), this ratio was of the order of 10^5 compared with a value of about 10^{-3} in the sound-to-light holograms.

Equation (5c) gives indication, as will be discussed later, of the reasons why sound holography has not been able to keep pace with optical holography.

SOUND HOLOGRAM RECORDING TECHNIQUES

The various techniques that have been used in sound hologram construction are summarized in Table I.

Table I.- Summary of Sound Image Detection Techniques

No.	Type of Detector	Detectable Threshold of Acoustic Power (approx.)
1	Photographic Emulsions	1 watt/cm^2 (refs. 2-3)
2	Thermoplastics	0.1 watt/cm^2 (ref. 4)
3	Liquid Surface Deformation	10^{-3} watt/cm^2 (ref. 5)
4	Electronic Methods	$\leq 10^{-8}$ watt/cm^2 (refs. 6-7)

Owing to high power requirements for methods 1 and 2, the discussion will be confined to methods 3 and 4.

Figure 2 shows general technique for sound imaging using the liquid-gas interface as the recording medium. The interference pattern is formed on the surface of the liquid. When a free liquid surface is exposed to an acoustic front, it adjusts itself to the acoustic pressure distribution. The pressure equation on the liquid-gas interface is (ref. 8):

$$\rho g h = 2P + \gamma \nabla^2 h \qquad (6)$$

where $P = |p|^2 / 2\rho v$

p = acoustic pressure amplitude

v = velocity of sound in the liquid

γ = surface tension of the liquid

h = vertical surface deformation height

ρ and g have usual significance.

Green (ref. 9) has investigated this liquid surface interaction with the sound field and concluded that it acts as a low-pass filter. The surface pattern is photographed to form a conventional hologram.(*) The hologram is suitably demagnified to take account of the fact that the interrogating light signal has much smaller wavelength than the investigating acoustical signal. To increase the sensitivity of this method of recording, the liquid is often wetted by a wetting agent with low surface tension. However, as indicated in Table I, this technique requires rather high intensity levels (at least for the reference beam) for successful direct playback and also suffers from other aberrations introduced by the physical processes involved. This technique will not receive any further consideration in this report.

The most sensitive techniques for recording acoustic holograms involve the use of piezoelectric crystals. Figure 3 shows a typical experimental arrangement. In this arrangement, the direct and scattered ultrasound waves impinge on the piezoelectric receiver producing a voltage distribution whose amplitude at any point is directly related to the resultant acoustic amplitude resultant acoustic amplitude at that point. The voltage distribution at the receiver surface modulates the secondary electron emission caused by a scanning electron beam. The resulting signal, after suitable amplification, is displayed on a television monitor. The television screen is photographed for subsequent conventional reconstruction. The main objections to this system are:

1. Limited resolution

2. Lack of simultaneous display of reconstructed image

(*)By illuminating the surface pattern with a laser beam, one may immediately reconstruct the underwater object. (The reconstructed image will be distorted as indicated in the Appendix.)

Using the Rayleigh criterion, the resolution, X, for a system is given by

$$X = 1.22\ D\left(\frac{\lambda}{a}\right) \tag{7}$$

where D = object-receiver distance

λ = investigating wavelength

a = aperture of the receiver

The aperture, in this technique, is limited by the maximum angle of detection of the receiver.* For quartz, this critical angle is of the order of 18°, thereby limiting the $\frac{D}{a}$ value to $\left(\frac{\text{Cot } 18^\circ}{2}\right)$. The aperture is further limited† by the fact that the receiver thickness is about half the wavelength of the ultrasound in quartz for a crystal operated at the resonance point. The limited aperture limits the size of the objects that can be investigated by this technique.

Another technique involves the use of direct interaction of light waves with the sound field (ref. 11). The diffracted light rays carry an image of the sound fields. Yet another technique of constructing acoustic holograms uses a microphone as the receiver. The microphone mechanically scans the acoustic fields at the hologram plane. The output signals from the microphone are amplified and used to light a lamp which is focused on a photographic film (ref. 12). In some cases, the microphone output modulates the scanning spot of a CRT whose face can be photographed to get a hologram.

One major point of difference between acoustic holography and optical holography stems from the fact that the acoustic waves can be detected by linear transducers whereas only squared-law detectors are usable with optical waves. As a result of this difference, it is not necessary to use

---

*This limitation has recently (ref. 10) been circumvented for the reference beam by the use of an electrically generated reference beam in the construction of the hologram instead of the acoustic reference beam. In the modified arrangement, it is possible to place the object closer to the receiver and use normal incidence of the object beam on the receiver, thus avoiding losses due to reflection. There is no limitation on the electrically generated reference beam. Such a scheme also reduces distortion in the reconstructed image.

†For a fixed thickness, mechanical safety limits the physical size of the crystal.

a reference beam in acoustic imaging. Such a reference beam can be simulated electronically to fall at any angle on the hologram plane.*

DISCUSSION OF ACOUSTIC HOLOGRAM RECONSTRUCTION TECHNIQUES

As has been indicated earlier, visual observation of acoustical image requires the use of visible radiation for interrogating an acoustical hologram. All existing techniques attain this objective by first making an acoustical image and then interrogating it at a later stage with visible light. This approach necessarily lacks simultaneity. It is essential for three-dimensional, real-time display that the imtermediate recording stage be eliminated. A technique which may eliminate the intermediate stage is described below. For instance, in the case of electronic recording method described earlier, it should be possible to precede the regular TV screen with an additional screen coated with an appropriate phosphor which is such that its optical transmission at any point is directly related to the incident electron beam intensity at that point. (Such a phosphor - called scotophor - has been discussed in ref. 14.) A built-in laser beam of appropriate wavelength could interrogate the additional screen at the same time when the piezoelectric receiver output is displayed on it. Upon electron bombardment, the scotophor atoms get excited leading to increased absorption of the interrogating laser beam passing through it. Under such circumstances, the additional screen behaves essentially as a hologram transparency. This arrangement would lead to an instantaneous optical display of the acoustical image on the regular TV screen. (See figure 4 for suggested technique.)

Another fruitful approach, which was recently reported in progress in England (ref. 15), concerns the development of piezoelectric electroluminescent sonic detectors. In this technique, piezoelectric voltages with some additional simulation could excite a phosphor to provide a visual display of the acoustic hologram.

In addition to lack of simultaneous display, the current sonic image detection techniques suffer from distortion attendant on demagnification resulting from the difference between the investigating and the interrogating wavelengths. The reproduction of a distortionless image calls for a match between the demagnification factor in the hologram and the ratio λ(inspection)/λ(interrogation). (See Appendix.) In the field of medical diagnosis where megahertz range frequency sound waves are used, there is no reason why the conventional visible optical interrogating wave cannot be replaced by an appropriate IR laser beam. (Table II lists various suitable laser transitions.) There are two potential advantages of this approach. The first, of course, arises from the fact that lateral and axial magnifications come closer to each other - a requirement for 3-D display. But a potentially more important advantage stems from the fact that it may

*Recently, Metherell et al. (ref. 13) have demonstrated that in true acoustical holography - temporal reference holography - one does not need a reference wave. The object wave already has the necessary image information.

Table II.- A List of Appropriate Spectral Lines for use in IR Imaging of Acoustical Holograms

Emitter Gas Atom or Molecule	λ(air), micrometers	Spectral Transition (Racah Notation)	Reference
Neon	20.480 μm	$6p[1/2]_0 - 5d[1/2]^0_1$	16
	31.553 μm	$6p[3/2]_2 - 5d[5/2]^0_3$	16
	41.741 μm	$6p[1/2]_1 - 5d[3/2]^0_2$	17
	50.705 μm	$7p[3/2]_2 - 6d[3/2]^0_2$	18
	68.329 μm	$7p[1/2]_1 - 6d[3/2]^0_2$	19
	89.859 μm	$8p[5/2]_3 - 7d[7/2]^0_3$	18
Argon	26.944 μm	$4d'[3/2]^0_2 - 4f[5/2]_3$	16
Xenon	18.506 μm	$5d'[3/2]^0_2 - 4f[5/2]_3$	16
CO_2	10.365 μm	R(4)	20
	10.440 μm	P(4)	

be possible to develop IR phosphors, which after suitable activation, emit in the visible range when exposed to IR in the high micron range. Such phosphors already exist (refs. 21 and 22) for use with 1-micron-range radiation (see figure 5(a)). Such phosphors need to be developed for wavelengths in the range 1-20 microns.* The concept of sensitizer (pump) ions coupled with the activator ions in a high purity semiconductor crystal is suggested as a potentially fruitful approach in this context. (See figure 5(b) for conceptual details.) Thus it appears that the use of IR interrogating laser beams, coupled with the IR → visible phosphors, may eliminate the major obstacle in the development of sound holography. In this connection, the use of the easily available 10.44 microns CO_2-laser beam for reconstructing acoustical holograms is recommended.

CONCLUDING REMARKS

Sound photography has long suffered for want of adequate recording techniques. Recent developments in optical holography, however, have spurred renewed interest in the visualization of sound fields. At present, it appears that sound holography has valid applications in two important areas: (1) Ultrasonic holography for medical purposes and for nondestructive materials research. The use of ultrasound here is dictated by the requirement that details of the object being observed must be larger than the sound wavelength.** (2) Underwater imaging for oceanography. These systems require lower frequencies than those needed in medical applications and nondestructive testing. Powerful coherent acoustic sources are presently available and the loss of coherence in water becomes serious only for very large pathlengths. It is, therefore, expected that with the development of proper distortionless viewing devices, sound holography will come into widespread usage in underwater exploration.

A discussion of the currently used techniques of recording and reconstructing sound holograms has brought out two major areas where further research is needed. One of these deals with the implications of the difference between the inspecting and interrogating radiations. For real-time, distortionless, sound viewing, it is recommended that infrared radiation of

---

*The energy content of a 20-micron photon is about 0.0625 eV (compared with a room temperature KT value of 0.025 eV). At longer wavelengths, the phosphors will have to be cooled to keep the KT value well below the photon energy.

**Ultrasound propagates at a speed of about 1.5 km/sec in soft tissue structures and its attenuation coefficient for wavelengths of the order of a fraction of a millimeter is small enough to permit medical diagnosis. Reasonable echo information is expected from soft tumerous tissues to enable early cancer detection by means of acoustical holography.

wavelength comparable to the inspecting sound waves be used. The infrared images can be viewed with (IR → visible) converter phosphors. The second area involves the real-time display of the visible image of the acoustically-inspected object at low sound levels such as are used in medical diagnosis. In this connection attention has been drawn to the need for a phosphor screen which is such that its optical transmission at any point is directly related to the incident electron beam intensity at that point. Such a screen, coupled with an acoustical camera, can enable instantaneous sound wave reconstruction.

REFERENCES

1. Gabor, D.: Nature 161, 777, 1948.

2. Bennett, G. S.: J. Acoust. Soc. Am. 24, 470-474, 1952.

3. Burger, H. and Kraska, I. R.: J. Acoust. Soc. Am. 34, 518-519, 1962.

4. Young, J. D. and Wolfe, W. E.: Appl. Phys. Letters 11, 294-296, 1967.

5. Rozenberg, L. D.: Soviet Physics - Acoustics 1, 105-116, 1955.
Pigulevskii, E. D.: Soviet Physics - Acoustics 4, 359-365, 1958.

6. Burger, H. and Dickens, R. E.: Argonne National Laboratory, Report ANL-6680, 1963.

7. Smyth, C. N.; Poynton, F. Y.; and Sayers, J. F.: Proc. IEEE, 110, 16, 1963. Green, P. S.: Lockheed Research Laboratory, Report AD-656-091 (6/29/67).

8. Mueller, R. K. and Sheridan, N. K.: App. Phys. Let. 9, 328, 1966.

9. Green, P. S.: Lockheed Research Laboratory, Report 6-77-67-42 (Sept. 1967).

10. Mueller, R. K.; Maron, E.; and Fritzler, D.: Appl. Phys. Let. 12, 394, 1968.

11. Korpel, A.: Appl. Phys. Let. 9, 425, 1966.

12. Matherell, A. F.; El-Sum, H. M. A.; Dreher, J. J.; and Larimon, L.:
(a) J. Acoust. Soc. Am. 42, 733, 1967. (b) Phys. Let. 24A, 547, 1967.
(c) Appl. Phys. Let. 10, 277, 1967.

Preston, K. and Krenzer, J. L.: Appl. Phys. Let. 10, 150, 1967.

13. Metherell, A. F., Spinak, S.; and Pisa, E. J.: Appl. Optics 8, 1543, 1969.

14. Leverenz, H. W.: RCA Review Vol. 7, No. 2, pp. 199-239, 1946.

15. Burger, H.: Acoustic Holography, Vol. I. (Plenum Press, p. 45, 1969).

16. Faust, et al.: Phys. Rev. 133, A1477, 1964.

17. Patel, et al.: Phys. Letters 4, 18, 1964.

18. Patel, et al.: Proc. IEEE, 52, 713, 1964.

19. McFarlane, et al.: Proc. IEEE, 52, 318, 1964.

20. Patel, et al.: Phys. Rev. Let 12, 588, 1964.

21. Hewes, R. A. and Sarver, J. F.: Phys. Rev. 182, 427, 1969.

22. Van Uitert, L. G.; Singh, S.; Levinstein, H. J.; Johnson, L. F.; Grodkiewicz, W. H.; and Geusic, J. E.: App. Phys. Let. 15, 53, 1969.

23. Meier, R. W.: J. Opt. Soc. Am. 55, 987, 1965.

24. Leith, E. N.; Upatnieks, J.; and Haines, K. A.: J. Opt. Soc. Am. 55, 981, 1965.

APPENDIX

DISTORTIONS IN SOUND IMAGE RECONSTRUCTION

Let Ψ_r, Ψ_o, and Ψ_c be the amplitudes of the reference, the object and the interrogating wavefronts and let λ_r, λ_o, and λ_c be the corresponding wavelengths. If the sound hologram transparency is such that the amplitude transmission is proportional to the intensity, the emergent wavefront, Ψ, is given by:

$$\Psi = \Psi_c \left[|\Psi_o|^2 + |\Psi_r|^2 + \Psi_o^* \Psi_r + \Psi_o \Psi_r^* \right] \tag{1}$$

where Ψ (Real) $= \Psi_c \cdot \Psi_o^* \Psi_r$
Ψ (Virtual) $= \Psi_c \cdot \Psi_o \Psi_r^*$

} This choice is determined by the experimental conditions

From equation (1), it is obvious that

$$\begin{aligned} \phi(\text{Real}) &= \phi_c - \phi_o + \phi_r \\ \phi(\text{Virtual}) &= \phi_c + \phi_o - \phi_r \end{aligned} \tag{2}$$

where the ϕ's give corresponding phases within the hologram plane relative to the phase at the origin.

Determination of the phase, ϕ (refs. 23-24)

Consider an object point $A(x_o, y_o, z_o)$ in a frame of reference centered in the hologram and let the hologram be in the x-y plane. Then the phases, ϕ, are easily calculated as follows:

$$\begin{aligned} \phi_o &= \frac{2\pi}{\lambda_o} \left\{ \left[(x' - x_o)^2 + (y' - y_o)^2 + (z' - z_o)^2 \right]^{\frac{1}{2}} - \left[x_o^2 + y_o^2 + z_o^2 \right]^{\frac{1}{2}} \right\} \\ &= \frac{2\pi}{\lambda_o} z_o \left[1 + \frac{x'^2 + x_o^2 + y'^2 + y_o^2 - 2x'x_o - 2y'y_o}{2z_o^2} - 1 - \frac{x_o^2 + y_o^2}{2z_o^2} \right] \\ &= \frac{2\pi}{\lambda_o} \left(\frac{x'^2 + y'^2 - 2x'x_o - 2y'y_o}{2z_o} \right) \end{aligned} \tag{3}$$

$$\phi_r = \frac{2\pi}{\lambda_r}\left(\frac{x'^2 + y'^2 - 2x'x_r - 2y'y_r}{2z_r}\right)$$

$$= \frac{2\pi}{\lambda_o}\left(\frac{x'^2 + y'^2 - 2x'x_r - 2y'y_r}{2z_r}\right) \quad \because \lambda_o = \lambda_r \tag{4}$$

$$\phi_c = \frac{2\pi}{\lambda_c}\left(\frac{x^2 + y^2 - 2xx_c - 2yy_c}{2z_c}\right) \tag{5}$$

x' and y' in equations (3) and (4) are the coordinates in the hologram as recorded. Before reconstruction, they were transformed to x, y because of the use of wavelength $\lambda_c \neq \lambda_o$.

We have $m_1 = \frac{\lambda_c}{\lambda_o}$ and $m_2 = \frac{x}{x'}$

Substituting the appropriate values of ϕ in equation (2), we get:

$$\phi_R(\text{First Order}) = \phi_c - \phi_o + \phi_r = \frac{2\pi}{\lambda_c}\left\{\frac{x^2 + y^2 - 2xx_c - 2yy_c}{2z_c}\right.$$

$$- \frac{x'^2 + y'^2 - 2x'x_o - 2y'y_o}{2z_o}$$

$$\left. + \frac{x'^2 + y'^2 - 2x'x_r - 2y'y_r}{2z_r}\right\}$$

$$\phi_{\text{Real}}(\text{First Order}) = \frac{2\pi}{\lambda_c}\left\{\frac{x^2 + y^2}{2}\left(\frac{1}{z_c} - \frac{m_1}{m_2^2 z_o} + \frac{m_1}{m_2^2 z_r}\right) - x\left(\frac{x_c}{z_c} - \frac{m_1 x_o}{m_2 z_o} + \frac{m_1 x_r}{m_2 z_r}\right)\right.$$

$$\left. - y\left(\frac{y_c}{z_c} - \frac{m_1 y_o}{m_2 z_o} + \frac{m_1 y_r}{m_2 z_r}\right)\right\} \tag{6}$$

If this expression corresponds to the phase for a gaussian sphere, we get

$$\phi_{\text{Real}}(\text{First Order}) = \frac{2\pi}{\lambda_c}\left(\frac{x^2 + y^2 - 2xx'' - 2yy''}{2z_R}\right)$$

$$\text{where} \quad x'' = \frac{m_2^2 x_c z_o z_r - m_1 m_2 x_o z_c z_r + m_1 m_2 x_r z_c z_r}{m_2^2 z_o z_r - m_1 z_c z_r + m_1 z_c z_o} \tag{7}$$

$$\text{and} \quad z_R = \frac{m_2^2 z_c z_o z_r}{m_2^2 z_o z_r - m_1 z_c z_r + m_1 z_c z_o} \tag{8}$$

We will now use these values of x'' and z_R to calculate the magnification and compare it with the value obtained by using the imaging formula.

$$M(\text{Lateral}) = \frac{1}{\left(\frac{z_o}{f_R} - 1\right)} \tag{9}$$

$$\text{where} \quad \frac{1}{f_R} = \frac{1}{z_o} + \frac{1}{z_R} \tag{10}$$

$$= \frac{1}{z_o} + \frac{1}{z_c} - \frac{m_1}{m_2^2 z_o} + \frac{m_1}{m_2^2 z_r} \tag{11}$$

Substituting the value of f_R in equation (9), we get

$$M(\text{Lateral}) = -\left(\frac{m_2^2}{m_1}\right)\frac{1}{\left(1 - \frac{m_2^2 z_o}{m_1 z_c} - \frac{z_o}{z_r}\right)} \tag{12}$$

Using the values of x'' and z_R given in equations (7) and (8), one obtains

$$M(\text{Lateral}) = m_2\left(\frac{1}{1 - \frac{m_2^2}{m_1}\frac{z_o}{z_c} - \frac{z_o}{z_r}}\right) \tag{13}$$

Equations (12) and (13) differ by a factor of $\frac{m_2}{m_1}$. These equations will give identical results only if $m_1 = m_2$. Similarly, the value of M(Long) obtained by the two methods differ by a factor of $\frac{1}{m_1}$ indicating a compression factor of $\frac{1}{m_1}$ for the reconstituted image.

It now remains to be shown that if $m_1 = m_2$ the spherical aberrations in the reconstituted image is zero.

Spherical aberration, due to third order terms in Z in equations for ϕ, is given by

$$S = \frac{1}{z_c^3} - \frac{m_1}{m_2^4}\frac{1}{z_o^3} + \frac{m_1}{m_2^4}\frac{1}{z_r^3} - \frac{1}{z_R^3}$$

$$= \frac{m_1}{m_2^4}\left\{\left(\frac{m_1^2}{m_2^2} - 1\right)\left(\frac{1}{z_o^3} - \frac{1}{z_r^3}\right) - \frac{3m_1}{z_c}\left(\frac{1}{z_o^2} + \frac{1}{z_r^2}\right)\right.$$

$$\left. + 3\left(\frac{m_2^2}{z_c^2} - \frac{m_1^2}{m_2^2\, z_o\, z_r}\right)\left(\frac{1}{z_o} - \frac{1}{z_r}\right) + \frac{6m_1}{z_o\, z_r\, z_c}\right\} \tag{14}$$

For $z_r = z_c = \infty$, this reduces to

$$S = \frac{m_1}{m_2^4}\left(\frac{m_1^2}{m_2^2} - 1\right) \Big/ z_o^3 \tag{15}$$

Clearly $S = 0$ only if $m_1 = m_2$, i.e., the degree of demagnification of the hologram must match the ratio of $\frac{\lambda_c}{\lambda_o}$ for minimal spherical aberration. This condition also minimizes other distortions, such as coma and astigmatism. These results clearly indicate the desirability of making m_1 as close to unity as possible. One possibility that suggests itself involves the use of 10.5 microns CO_2 laser beam as the interrogating radiation and an acoustic beam of comparable wavelength as the investigating radiation, at least for medical diagnostic purposes.

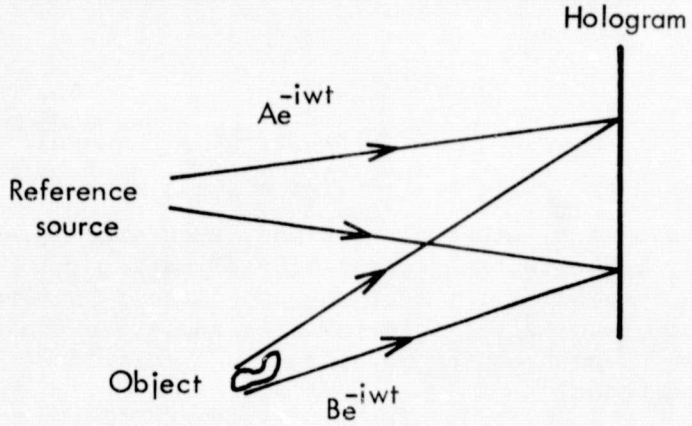

(a) - Construction of a hologram.

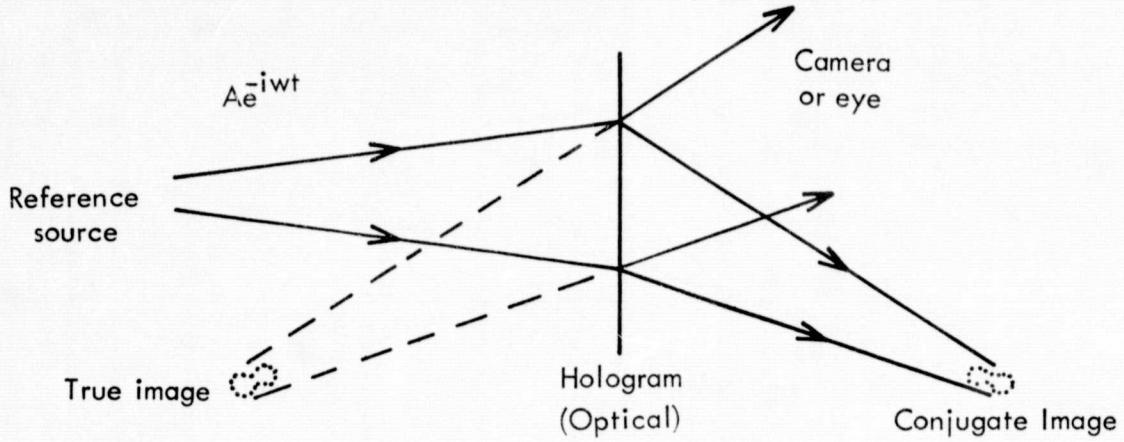

(b) - Re-constructing the image by illuminating the hologram with the reference beam alone.

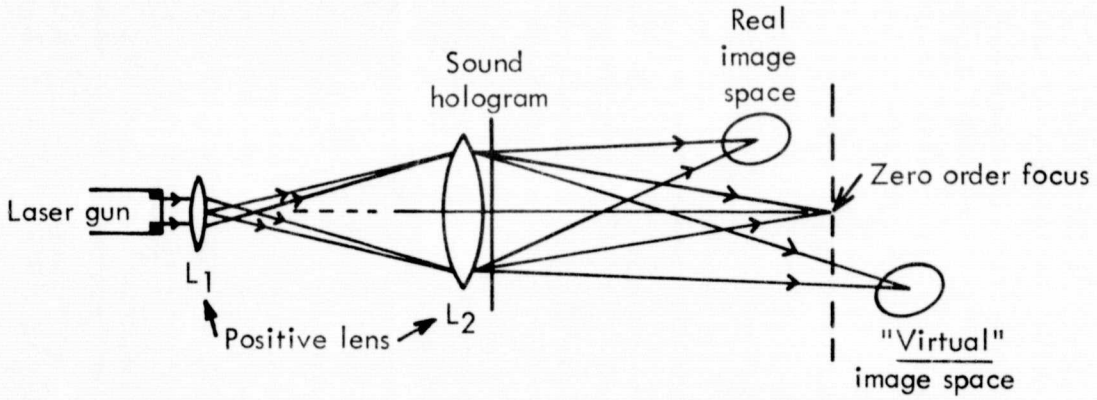

(c) - Re-constructing the image by using an interrogating radiation different from the two original beams.

Figure 1 - Hologram construction/reconstruction technique.

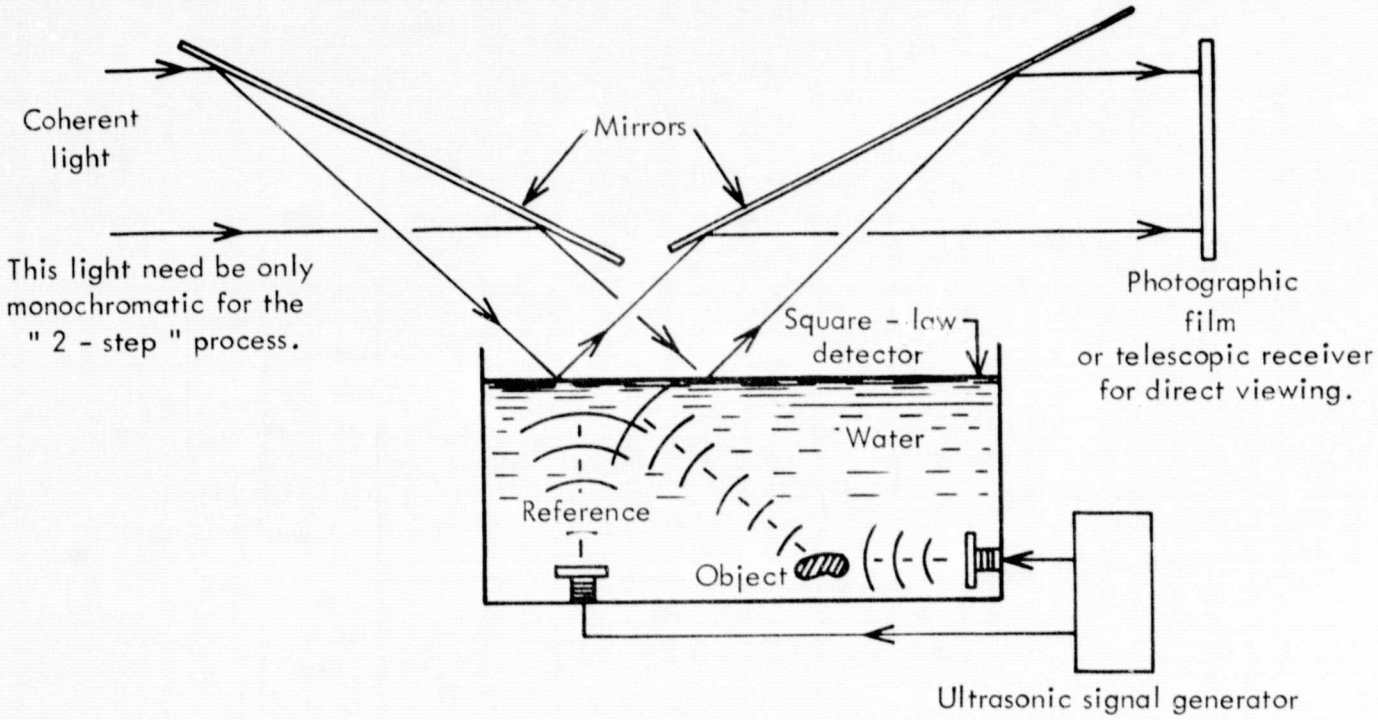

Figure 2. - Method of recording a liquid surface hologram. The parallel beam of coherent light, upon reflection from the deformed surface, produces a permanet record of the hologram.

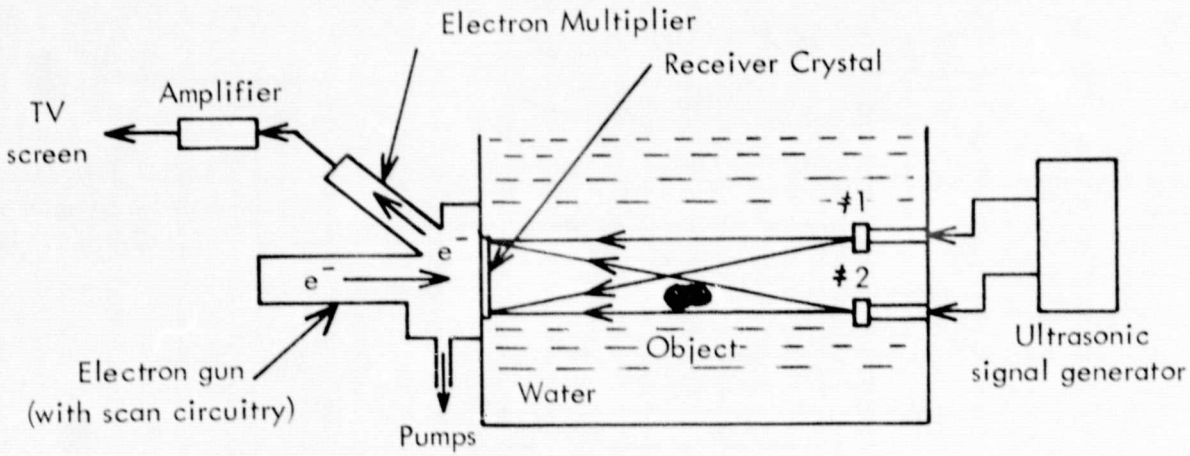

Figure 3. - Experimental set up for electronic sound hologram construction. The piezo-electric detector is scanned by an electron beam. The secondary electron beam from the detector is modulated by the acoustic field at the detector.

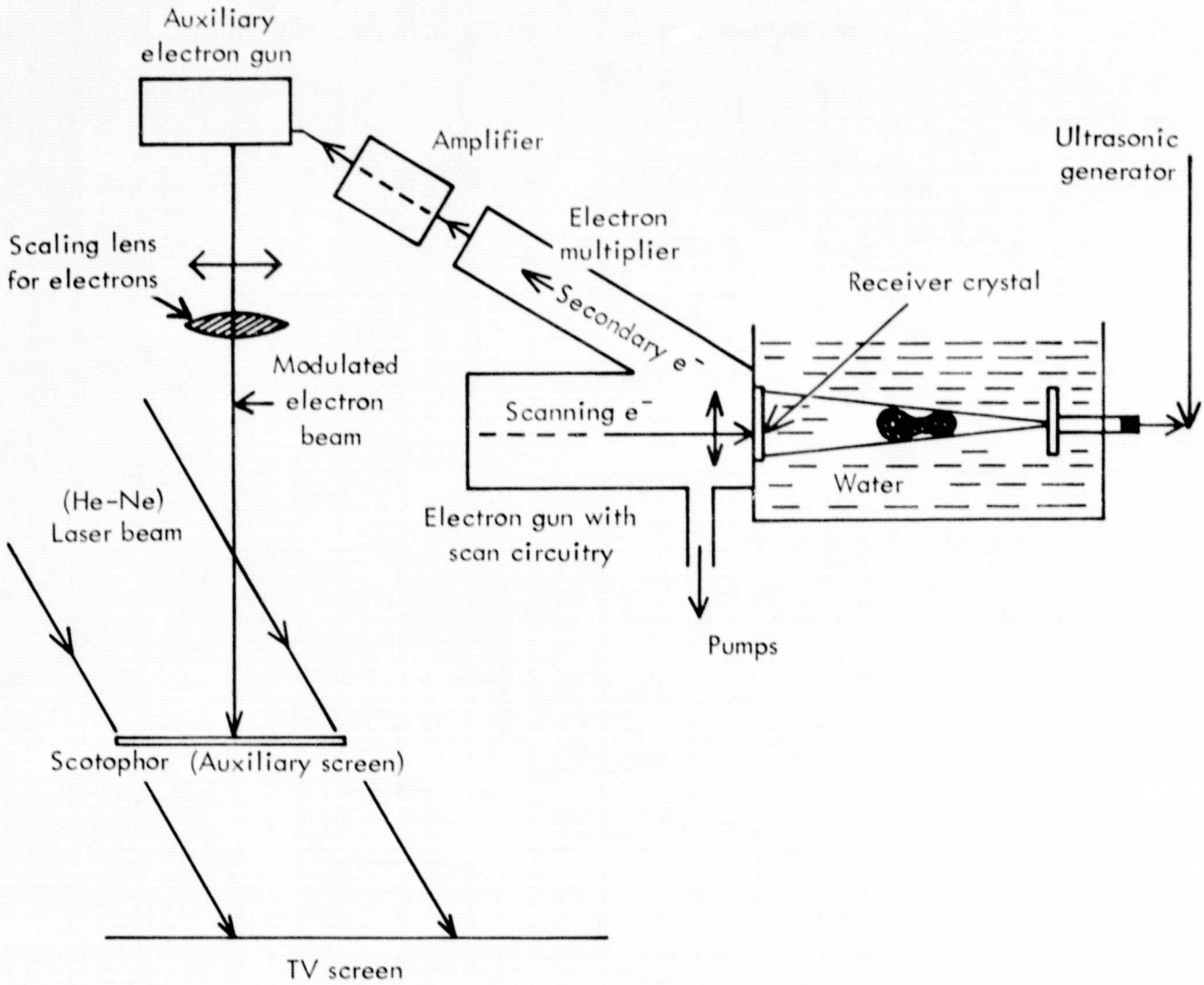

Figure - 4. Suggested arrangement for the variable impedance optical filter and the TV screen for simultaneous hologram reconstruction. The scanning electron beam on the receiver crystal and the modulated electron beam on the auxiliary screen move in unison. The electrostatic lens between the scotophor and the electron gun scales down the hologram appropriately.

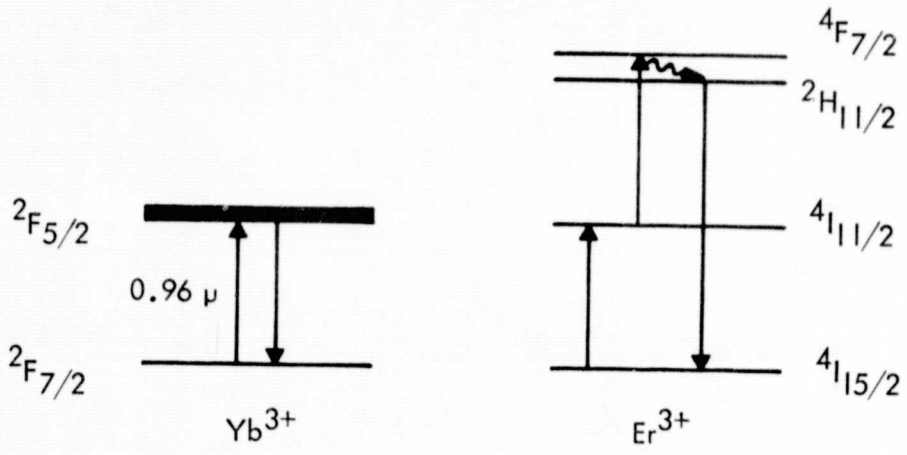

Figure - 5 - A. Infrared excitation processes for the visible luminescence of Er^{3+} in Yb^{3+} - sensitized (La F_3: Yb, Er). (After ref. - 21).

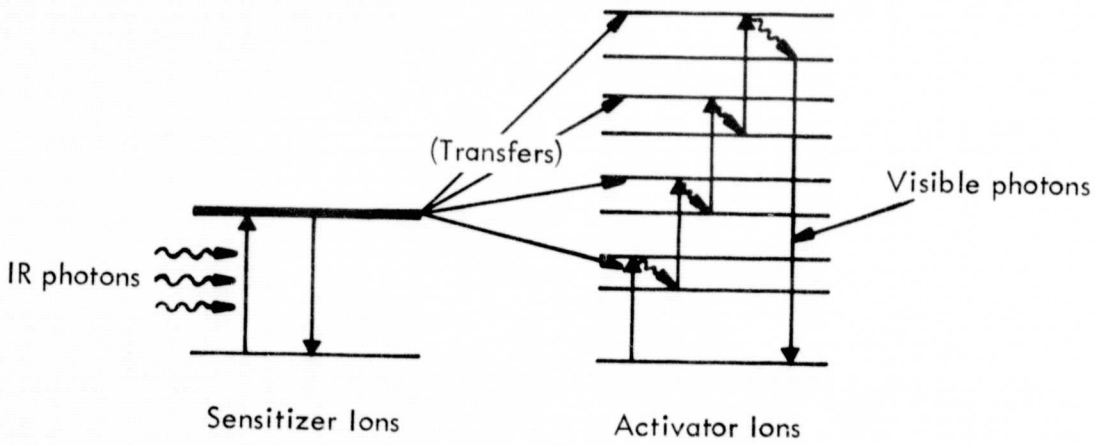

Figure - 5 - B. Suggested mechanism for IR→ visible emission phosphors.